# Quantum Chemical Study of Some Basic Organic Compounds as the Corrosion Inhibitors

Lana Omar Ahmed[1]*, Omer Kaygili[2], Niyazi Bulut[2], Rebaz Anwer Omer[3]

[1]Department of Physics, Faculty of Science and Health, Koya University, Koya KOY45, Kurdistan Region – F.R, Iraq
[3]Department of Chemistry, Faculty of Science and Health, Koya University, Koya KOY45, Kurdistan Region – F.R, Iraq
[1, 2]Department of Physics, Faculty of Science, Firat University, 23119 Elazig, Türkiye
* Corresponding author: E-mail: lana.omer@koyauniversity.org

## ABSTRACT

The corrosion inhibitor activities of 10 molecules (Benzene (C1), Phenol (C2), Toluene (C3), Benzoic acid (C4), Acetophenone (C5), Chlorobenzene (C6), Bromobenzene (C7), Benzaldehyde (C8), Naphthalene (C9), and Anthracene (C10) were investigated using quantum mechanical methods. The energy of the highest occupied molecular orbital ($E_{HOMO}$), the energy of the lowest occupied molecular orbital ($E_{LUMO}$), the energy bandgap ($E = E_{LUMO} - E_{HOMO}$), and the dipole moment ($\mu$) were all estimated in this study. The parameters mentioned can provide information about the corrosion efficiency of organic compounds. In addition, the density functional theory (DFT) was used to determine the geometry of the molecules as well as the electronic properties of the compounds. Physical parameters such as chemical hardness ($\eta$), softness ($\sigma$), and electronegativity ($\chi$) were determined using B3LYP/6-31G (d, p). As well as the quantum chemistry properties like the fraction of electrons transported ($\Delta N$) between the iron surface and the titled compounds have been calculated. This research also aimed to find which variables have a significant linear relationship with inhibitory performance. According to the results, the behavior of organic-based corrosion inhibitors is related to the effectiveness of good corrosion inhibitors and the quantum chemical parameters measured during this process. As a result, corrosion inhibitor behavior can be predicted without the need for an experiment.

## ARTICLE INFO

## 1. Introduction

Metals are protected against corrosion by corrosion inhibitors. Inhibitors are chemicals to a corrosive medium that delay or stop metal corrosion [1-5]. Corrosion processes are responsible for a large number of deaths, particularly in the manufacturing industry. The only way to deal with it is to discourage it, as is evident. Corrosion inhibitors are one of the most well-known and successful strategies in the industry for avoiding or reducing metal surface damage or oxidation [6-8].

Because of their outstanding anti-corrosive properties, inhibitors have long been utilized in industry. However, many of them came as a result of side effects, resulting in environmental damage. Therefore, scientists began to search for ecologically acceptable compounds, such as organic inhibitors [9-16]. As a result, organic coatings have long been recognized as a low-cost technique for preventing metal corrosion [17]. The majority of organic inhibitors work by adsorbing onto metal surfaces [18]. Organic inhibitor molecules can adsorb onto corroding metals either physically or chemically [19].

The performance of the inhibitor can be investigated experimentally and/or theoretically by computational chemistry. Weight loss, linear polarization, potentiodynamic polarization, electrochemical impedance spectroscopy (EIS), UV visible spectroscopy, scanning electron microscope (SEM), X-ray spectroscopy (EDX) [20], and cyclic

voltammetry [21] are commonly used to perform observations of corrosion inhibition efficiency and to check the inhibition mechanism. On the other hand, depending only on experimental approaches is costly, time-consuming, and hazardous to the environment [22]. For this reason, many researchers have been working in computational chemistry [1, 23-26].

Quantum chemical calculations are used to identify the structural characteristics of organic corrosion inhibitors that are associated with corrosion inhibition properties [23]. Density functional theory (DFT) is a quantum chemistry approach for measuring the electronic properties of molecules [27, 28] and analyzing inhibitor/surface connections in corrosion inhibition research. Different electronic characteristics derived from quantum chemistry techniques are employed for calculations of corrosion inhibition capabilities as well as to support experimental measurements [29-31].

In this study, the density functional theory (DFT) at 6-31G (d, p) basis set was used to examine the corrosion inhibiting properties of 10 molecules (Benzene (C1), Phenol (C2), Toluene (C3), Benzoic acid (C4), Acetophenone (C5), Chlorobenzene (C6), Bromobenzene (C7), Benzaldehyde (C8), Naphthalene (C9), and Anthracene (C10)). In addition, the parameters typically connected to inhibition efficiency are identified.

## 2.    Methodology

Chem. Bio Draw Ultra 14.0 was used to draw the structures of the molecules (Benzene, Phenol, Toluene, Benzoic acid, Acetophenone, Chlorobenzene, Bromobenzene, Benzaldehyde, Naphthalene, and Anthracene) (Figure 1). All computations were performed using the Gaussian 09 packages. With Gaussian 09 program allows users to do many computations [32-39]. The ten molecules first have been optimized. The DFT method is used to precisely determine the electronic characteristics of the structures by taking into consideration the electron density and producing the appropriate data over this electron density. B3LYP is well-liked for a variety of reasons. It was one of the first DFT approaches to outperform Hartree-Fock. B3LYP is often quicker than most Post-Hartree-FockHartree-Fock methods, and the results are usually similar. For a DFT approach, it is also rather robust. It is not as highly specified as other hybrid functionals on a more basic level [40, 41]. Furthermore, the Gaussian 09W software's hybrid function B3LYP, which is compatible with the workstation's capability, and 6-31G (d,p) [42-44] as the basis set were employed.

The total energy, the energy of the maximum occupied molecular orbital ($E_{HOMO}$), the energy of the lowest unoccupied molecular orbital ($E_{LUMO}$), energy difference $\Delta E$, dipole moment ($\mu$), ionization energy, electron affinity, chemical hardness ($\eta$), softness ($\sigma$), nucleophilicity ($\varepsilon$) index, electrophilicity ($\omega$) index, chemical potential (Pi), and electronegativity ($\chi$) have all been calculated. The transmitted electron fraction ($\Delta N$) between the copper surface and the molecules has been computed.
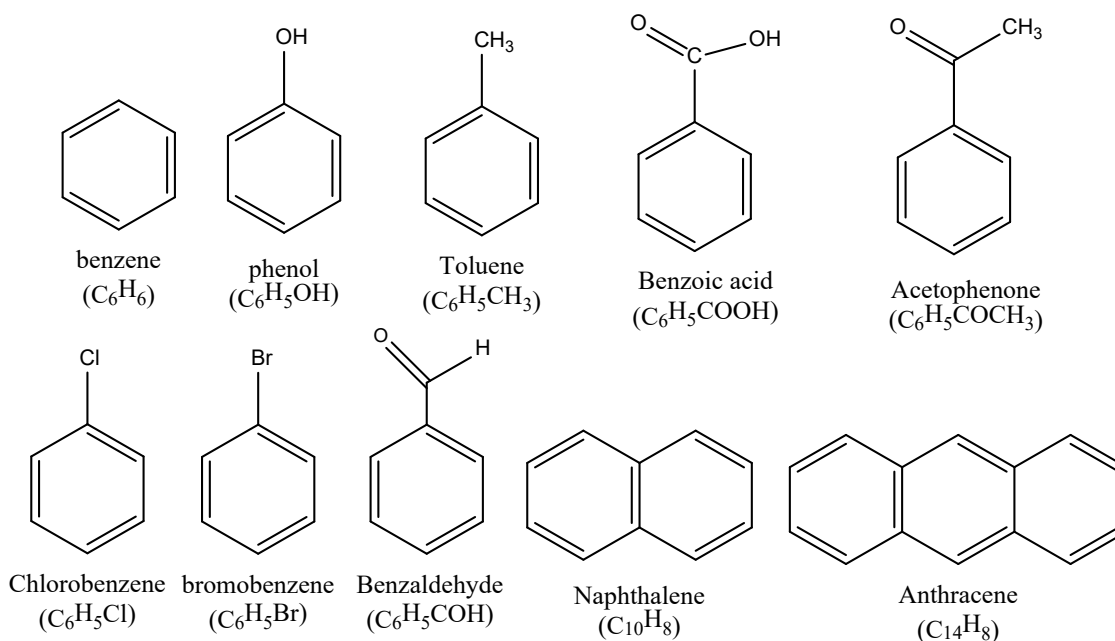


**Figure 1.** The structures of the molecules

## 3.    Result and Discussion

### 3.1    Structure optimization

The gas-phase geometry optimizations of all the structures (M1-10) were investigated by B3LYP (Fig. 2). Using 6-31G(d,p) basis set.
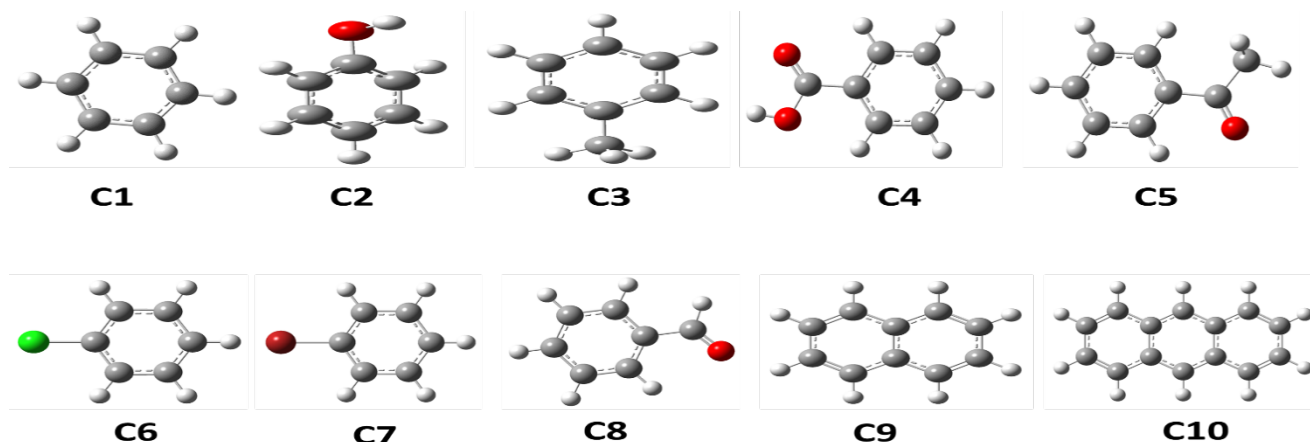


**Figure 2.** Geometrical optimization for all samples.

### 3.2    Inhibitor Parameters

Electronic structure identifiers have been derived from the electronic structure of the molecule and linked to the electronic structure [45]. The consistent electronic structural parameters, which contain $E_{HOMO}$, $E_{LUMO}$, $\Delta E$ gap, $\sigma$, $\chi$, Pi, $\sigma$, $\chi$, $\varepsilon$, $\mu$. The HOMO, LUMO, and $\mu$ data were resulting from the Gaussian outturn of the molecular profile. The existing equations in the literature can be used to calculate other parameters. The highest occupied and lowest unoccupied energy levels are defined as $E_{HOMO}$ and $E_{LUMO}$, respectively, and their values determine a material's reactivity or passivity. According to Koopman's theorem, $E_{HOMO}$ and $E_{LUMO}$ values of any chemical type are associated with its ionization energy and electron affinity values [46, 47]. The parameters $\Delta E$ [48], $\eta$, $\sigma$ [49], $\chi$, and Pi [50] are calculated according to the following equations:

$I = -E_{HOMO}$, $A = -E_{LUMO}$, $\Delta E = (E_{LUMO} - E_{HOMO})$, $\eta = (I - A) / 2$, $\sigma = I/\eta$,   $\chi = (I + A) / 2$, Pi = $-\chi$ , $\omega = Pi^2/2\eta$ and $\varepsilon = Pi * \eta$

The electrophilicity index ($\omega$) is a measure of energy depletion due to the overall electron flow between the transmitter and the receiver. The nucleophilicity index ($\varepsilon$) is a new chemical structure identifier. The number of electrons

transported between the inhibitor and the metal surface is calculated using the following equation ($\Delta N$) [19].

$$\Delta N = \frac{\chi metal - \chi inhibitor}{2.(\eta metal - \eta inhibitor)}$$

The value of $\chi$ and $\eta$ for the compound are calculated theoretically using DFT/B3LYP level with a 6-311G(d, p) basis set, while experimentally values for $\chi$ metal and $\eta$ metal were found from the literature [51] which was calculated by Pearson. According to Pearson, an individual metal's electron affinity (A) and ionization potential (I) are considered to be equal (I = A), and $\eta$ for a single metal value is assumed to be zero. Table 1 shows the electronic structural characteristics and total energy for the mentioned molecules. From Table 1 the HOMO and LUMO energies appear that they have a general tendency among them. HOMO is important for corrosion studies because it is related to electron-donating capacity. The inhibitory effect of inhibitor molecules increases with increasing HOMO values [52]. As a result, it affects the charge transfer mechanism along the metal surface, allowing for adsorption. The $E_{HOMO}$ ordered as follows:

C10>C9>C3>C2>C7>C6>C1>C5>C8>C4

According to the high EHOMO value, compound C10 has the highest inhibitory activity and compound C4 has the lowest inhibitory activity (Fig. 3). LUMO refers to the ability to accept electrons. A low $E_{LUMO}$ value indicates that the inhibitor can add a negative charge to the metal surface. The $E_{LUMO}$ ordered as shown below:

C2>C1>C3>C6>C7>C9>C4>C5>C10>C8

According to the $E_{LUMO}$ sequence, the LUMO energy of C10 has the lowest energy and the LUMO energy of C2 has the highest energy. It was determined that the C10 inhibitor was reactive by acting as a donor, and its inhibitor activity was therefore high. The C4 inhibitor has the lowest $E_{LUMO}$ and lowest $E_{HOMO}$ values. While low $E_{HOMO}$ inhibitors reduce metal reactivity, the metal inhibitor acts as a donor to the inhibitor. As a result, the inhibitor's activity decreases while the metal's reactivity increases. C10 molecule has the most effective corrosion inhibition based on HOMO-LUMO energies, see Figure 3.
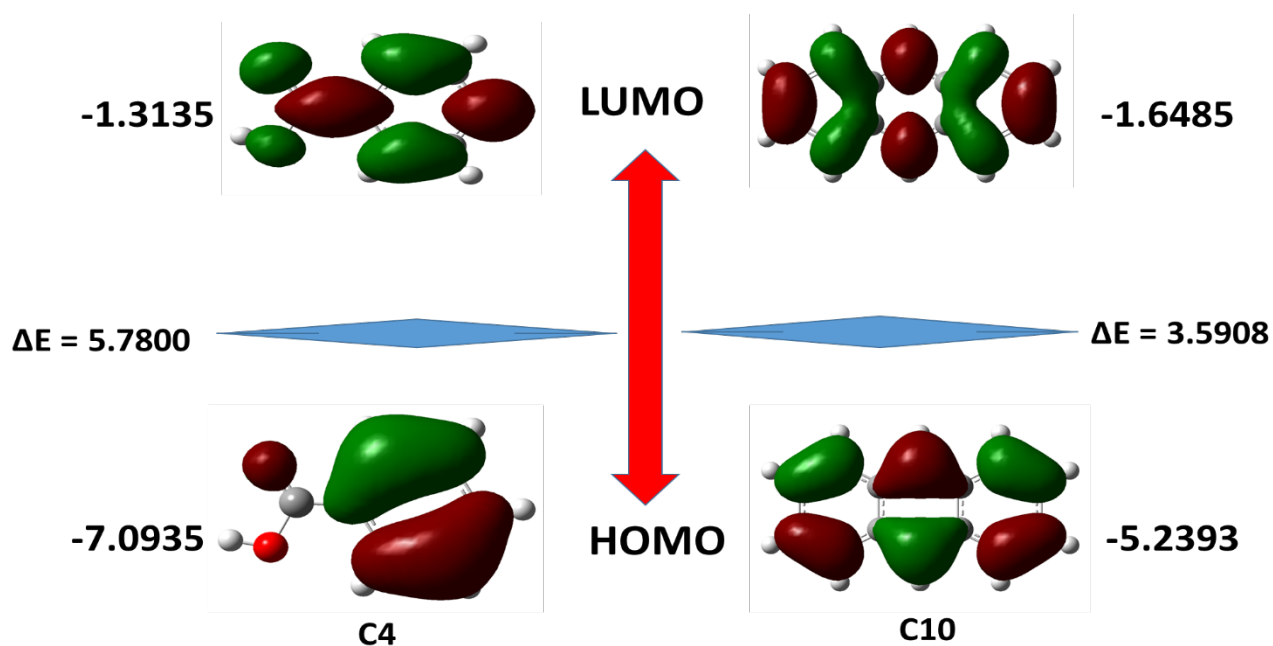


**Figure 3.** HOMO & LUMO energy levels for both Benzoic acid (C4), and Anthracene (C10).

The energy gap between $E_{HOMO}$ and $E_{LUMO}$ has a significant and clarity determining theoretical inhibition efficiency as well as static molecular reactivity. The sequence of the inhibitors was shown as follows based on the energy gap value:
C10>C9>C8>C5>C4>C7>C3>C6>C2>C1

The energy bandgap is a measure of the activity of the molecule. For inhibitor studies, it is critical to compare ΔE.

The lower value of the energy bandgap results in better inhibition efficiency. The lower ΔE value in corrosion inhibitors is determined by the $E_{HOMO}$ rather than the $E_{LUMO}$. Anti-corrosion agents can be made from inhibitor derivatives with high HOMO energy and low ΔE [52]. Given the above $E_{HOMO}$ and ΔE sequence, C10 will provide good inhibition activity depending on the highest HOMO energy value.

**Table 1.** The electron structure identifiers were calculated using the 6–31(d,p) basis of molecules in the gas phase at the DFT/B3LYP theory level.

| Parameters | Equations | Benzene | Phenol | Toluene | Benzoic Acid | Aceto phenone | Chloro benzene | Bromo benzene | Benzaldehyde | Naphthalene | Anthracene |
|---|---|---|---|---|---|---|---|---|---|---|---|
| Total Energy (a.u) | | -232.2582 | -307.4722 | -271.5788 | -420.8354 | -384.9082 | -691.8529 | -2803.3617 | -345.5827 | -425.0630 | -617.8310 |
| μ (D) | | 0.0000 | 1.5635 | 0.3423 | 1.9154 | 2.9830 | 1.9180 | 1.8099 | 3.2818 | 0.0000 | 0.0015 |
| ELUMO (eV) | | -0.0729 | -0.0188 | -0.1222 | -1.3135 | -1.4809 | -0.3646 | -0.3655 | -1.7260 | -0.9793 | -1.6485 |
| EHOMO | | -6.7194 | -6.4794 | -6.4121 | -7.0935 | -6.7259 | -6.7139 | -6.5901 | -6.9447 | -5.8026 | -5.2393 |

| (eV) | | | | | | | | | | | |
|---|---|---|---|---|---|---|---|---|---|---|---|
| ΔE (eV) | | 6.6464 | 6.4606 | 6.2900 | 5.7800 | 5.2450 | 6.3493 | 6.2247 | 5.2186 | 4.8233 | 3.5908 |
| I (eV) | I = -EHOMO | 6.7194 | 6.4794 | 6.4121 | 7.0935 | 6.7259 | 6.7139 | 6.5901 | 6.9447 | 5.8026 | 5.2393 |
| A (eV) | A = -ELUMO | 0.0729 | 0.0188 | 0.1222 | 1.3135 | 1.4809 | 0.3646 | 0.3655 | 1.7260 | 0.9793 | 1.6485 |
| χ (eV) | χ = (I + A)/2 | 3.3961 | 3.2491 | 3.2672 | 4.2035 | 4.1034 | 3.5393 | 3.4778 | 4.3354 | 3.3910 | 3.4439 |
| η (eV) | η = (I − A)/2 | 3.3232 | 3.2303 | 3.1450 | 2.8900 | 2.6225 | 3.1746 | 3.1123 | 2.6093 | 2.4116 | 1.7954 |
| σ (eV) | σ = 1/η | 0.3009 | 0.3096 | 0.3180 | 0.3460 | 0.3813 | 0.3150 | 0.3213 | 0.3832 | 0.4147 | 0.5570 |
| Pi (eV) | Pi = -χ | -3.3961 | -3.2491 | -3.2672 | -4.2035 | -4.1034 | -3.5393 | -3.4778 | -4.3354 | -3.3910 | -3.4439 |
| ω (eV) | ω = Pi2/2η | 1.7353 | 1.6340 | 1.6970 | 3.0570 | 3.2102 | 1.9729 | 1.9431 | 3.6016 | 2.3840 | 3.3030 |
| ε (eV) | ε = Pi. η | -11.2861 | -10.4954 | -10.2752 | -12.1482 | -10.7612 | -11.2359 | -10.8240 | -11.3123 | -8.1778 | -6.1833 |
| ΔN | ΔN = (χmetal - χinhibitor) / 2. (ηmetal - ηinhibitor) | 0.5422 | 0.5806 | 0.5935 | 0.4838 | 0.5523 | 0.5451 | 0.5659 | 0.5106 | 0.7483 | 0.9903 |

Table 2 shows the atomic charge distributions on the inhibitor's molecular structure. Mulliken population analysis is a popular method for predicting the adsorption centers of inhibitor molecules (Table 2). Many researchers agreed that the presence of negatively charged heteroatoms increases the ability to adsorb on the metal surface by the donor-acceptor mechanism [53, 54]. As the result, the negatively charged in the center of the aromatic ring, C10 has an effective inhibitory effect. The aromatic ring has a denser red color, as seen in the MEP map in Figure 4. This can be interpreted as the C10 inhibitor being coordinately bound to the metal surface from these centers.

**Table 2.** Charge distribution on the atoms for each molecule.

| Benzene | Phenol | Toluene | Benzoic Acid | Aceto phenone | Chloro benzene | Bromo benzene | Benzaldehyde | Naphthalene | Anthracene |
|---|---|---|---|---|---|---|---|---|---|
| 1 C -0.083921 | 1 C -0.083078 | 1 C -0.087315 | 1 C -0.072757 | 1 C -0.074040 | 1 C -0.076274 | 1 C -0.084742 | 1 C -0.073778 | 1 C -0.092621 | 1 C -0.097884 |
| 2 C -0.083817 | 2 C -0.091047 | 2 C -0.084628 | 2 C -0.090006 | 2 C -0.091860 | 2 C -0.086499 | 2 C -0.078863 | 2 C -0.088063 | 2 C -0.128589 | 2 C -0.120643 |
| 3 C -0.083900 | 3 C -0.093222 | 3 C -0.113161 | 3 C -0.103092 | 3 C -0.117941 | 3 C -0.076274 | 3 C -0.091510 | 3 C -0.113867 | 3 C 0.101945 | 3 C 0.110050 |
| 4 C -0.083921 | 4 C 0.285433 | 4 C 0.102704 | 4 C 0.049768 | 4 C 0.051136 | 4 C -0.074744 | 4 C 0.055669 | 4 C 0.036810 | 4 C 0.102287 | 4 C 0.110043 |
| 5 C -0.083817 | 5 C -0.093222 | 5 C -0.113161 | 5 C -0.097000 | 5 C -0.095878 | 5 C -0.089429 | 5 C -0.091510 | 5 C -0.093975 | 5 C -0.128295 | 5 C -0.120666 |
| 6 C -0.083900 | 6 C -0.091047 | 6 C -0.084628 | 6 C -0.089414 | 6 C -0.087567 | 6 C -0.074744 | 6 C -0.078863 | 6 C -0.085367 | 6 C -0.092980 | 6 C -0.097881 |
| | 12 O -0.595143 | 12 C -0.374314 | 12 C 0.546772 | 12 C 0.375292 | 12 Cl -0.020699 | 12 Br -0.127018 | 12 C 0.257623 | 10 C -0.128213 | 7 C -0.209498 |
| | | | 13 O | 13 O | | | 14 O | 11 C | 8 C |

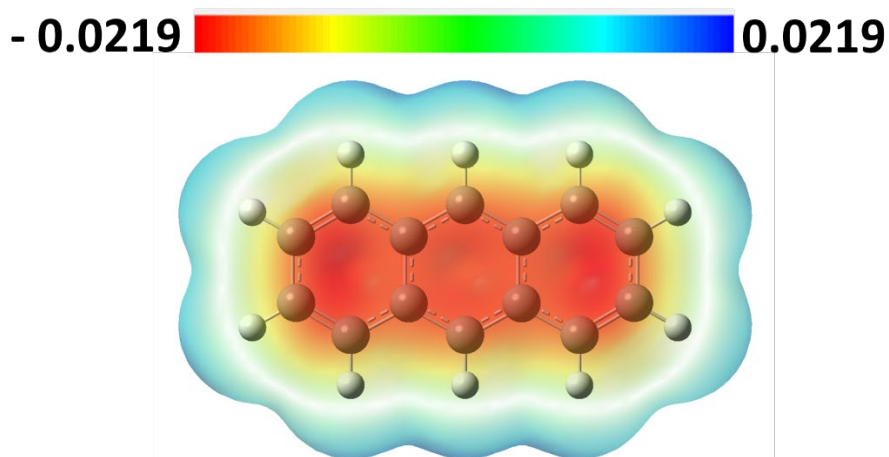| | | | | | | -0.425203 | -0.128707 | -0.209489 |
|---|---|---|---|---|---|---|---|---|
| | | -0.531308 | -0.468547 | | | | | |
| | | 15 O | 14 C | | | | | |
| | | -0.466598 | -0.385007 | | | 14 C -0.092621 | 9 C 0.110006 | |
| | | | | | | 15 C -0.092937 | 10 C 0.110076 | |
| | | | | | | | 11 C -0.120682 | |
| | | | | | | | 13 C -0.097872 | |
| | | | | | | | 14 C -0.097903 | |
| | | | | | | | 15 C -0.120635 | |

C: is the carbon number.



**Figure 4.** MEP map for Anthracene (C10)

The η and σ are two additional important parameters that provide information about an inhibitor's stability, reactivity, and inhibitor activity. The letters η and σ of inhibitors are arranged as follows:

η     C1>C2>C6>C3>C7>C4>C5>C8>C9>C10

σ     C10>C9>C8>C5>C4>C7>C3>C6>C2>C1

Because the organic chosen as an inhibitor acts as a Lewis base, and soft inhibitors are more reactive than hard inhibitors, they are better corrosion inhibitors [55]. In this case, the C10 inhibitor with high $E_{HOMO}$ and low $\Delta E$ had high softness and low hardness values. The values η and σ indicate that the C10 inhibitor has the most potent inhibitory effect.

Electronegativity (χ) and chemical potential (Pi) are two additional parameters used to calculate inhibitor activity. The χ calculated inhibitor values provide information on how the coordinated covalent bond between the metal and the inhibitor is formed [52]. The χ sequenced as follows:

C8>C4>C5>C6>C7>C10>C1>C9>C3>C2

The corrosion inhibition activity of molecules designed as inhibitors on iron metal was investigated in this study. The χ values calculated for the inhibitors in Table 1 were found to be lower than the experimental χ value for the iron metal. As a result, the iron metal will form bonds by absorbing electrons from the inhibitor compound. When we look at the χ sequence, the C10 and C9 inhibitors with the lowest χ value compared with another molecule will be the most effective corrosion inhibitor. The inverse of electronegativity is Pi. The molecules with high chemical potential will have high activity against other molecules, whereas the molecules with low potential will provide low activity [56]. C10 and C9, as shown in Table 1, are the most active inhibitors.

The $\omega$ and $\varepsilon$ indices are important parameters in corrosion inhibitor activity. The $\omega$ index denotes an inhibitor molecule's ability to accept electrons. The $\varepsilon$ index indicates the inhibitors' ability to donate electrons. The inhibition activity increases as the $\omega$ or $\varepsilon$ values decrease. The theoretical inhibition efficiency sequence in this study, according to $\omega$ and $\varepsilon$, is as follows:

$\omega$　C8>C9>C10>C5>C4>C6>C7>C1>C3>C2

$\varepsilon$　C10>C9>C3>C2>C5>C7>C6>C1>C8>C4

The calculated $\omega$ value of the C10 inhibitor decreased, and the $\varepsilon$ value increased, as shown in the sequence. The C10 inhibitor has the most effective inhibitory effect with $\omega$ and $\varepsilon$ values by the other parameters.

When the $\Delta N$ [19] values for iron and metal inhibitors are compared (Table 1), it can be concluded that the C10 molecule transfers more electrons to the iron metal, making it a more effective inhibitor.

The dipole moment is another parameter that has been shown in Table 1. However, no clear link between $\mu$ and inhibition activity has been found in the literature. According to certain studies, the activity of molecules with higher $\mu$ values leads to better inhibition, whereas other studies claim that the inhibition effect increases with decreasing $\mu$ value. The C10 inhibitor has a low dipole moment, which is consistent with the other parameters. This can be interpreted as better metal surface coverage at low $\mu$ values.

## 4.　Conclusion

The inhibitory activity of ten organic-based compounds was theoretically investigated in this study using the Gaussian package program. According to the results, $E_{LUMO}$ values of inhibitors with high $E_{HOMO}$ values were also found to be high. As a result, it was determined that the C10 inhibitor was reactive by acting as a donor, and as a result, its inhibitor activity was high. Inhibitor derivatives with high $E_{HOMO}$ and low $\Delta E$ can be used as anti-corrosion agents. Given the $E_{HOMO}$ and $\Delta E$ sequence, compound C10 will provide good inhibition activity depending on the highest value of $E_{HOMO}$. When the Mulliken atomic charges of the C10 inhibitor are examined, it can be stated that the electronegative atoms have a significant effect on the inhibition activity. The negatively charged atoms have HOMO centers on them, and from these centers, the inhibitor can be bound to the metal surface. The most active region in the MEP map can be seen around the ring. The calculated $\eta$, $\sigma$, $\chi$, Pi, $\omega$, and $\varepsilon$ parameters support the conclusion that the C10 inhibitor has the most effective corrosion inhibition effect. The lower $\chi$ the inhibitor value, the more the iron metal will form a bond by taking electrons from the inhibitor compound, and the higher the $\Delta N$ value,

the more the inhibitor will be adsorbed to the metal surface and the corrosion inhibition effect will increase. It can be interpreted as the C10 inhibitor, which is included in the study, being better at covering the metal surface at low dipole moment values, even though a clear conclusion about the dipole moment is not found in the literature. It is discovered that there is a close relationship between the activity of organic-based corrosion inhibitors with good corrosion inhibitor activity and the process's calculated quantum chemical parameters. One of its most significant advantages is that the studied structure can be changed based on calculations. The C10 compound has effective corrosion inhibition properties and thought to be more effective if the number of rings in other molecules' structures will be increased.

## References

1. L. AHMED and O. Rebaz, 1H-Pyrrole, Furan, and Thiophene Molecule Corrosion Inhibitor Behaviors. Journal of Physical Chemistry and Functional Materials, 2021. 4(2): p. 1-4.

2. M. Hegazy, et al., Synthesis, surface properties and inhibition behavior of novel cationic gemini surfactant for corrosion of carbon steel tubes in acidic solution. Journal of Molecular Liquids, 2015. 211: p. 126-134.

3. S. Deng and X. Li, Inhibition by Ginkgo leaves extract of the corrosion of steel in HCl and H2SO4 solutions. Corrosion Science, 2012. 55: p. 407-415.

4. N. Muthukumar, et al., 1-Aminoanthraquinone derivatives as a novel corrosion inhibitor for carbon steel API 5L-X60 in white petrol–water mixtures. Materials chemistry and physics, 2009. 115(1): p. 444-452.

5. R. Saratha and V. Vasudha, Inhibition of mild steel corrosion in 1N H2SO4 medium by acid extract of Nyctanthes arbortristis leaves. E-journal of Chemistry, 2009. 6(4): p. 1003-1008.

6. M. Al-Otaibi, et al., Corrosion inhibitory action of some plant extracts on the corrosion of mild steel in acidic media. Arabian Journal of Chemistry, 2014. 7(3): p. 340-346.

7. I. Obot, N. Obi-Egbedi, and S. Umoren, Antifungal drugs as corrosion inhibitors for aluminium in 0.1 M HCl. Corrosion Science, 2009. 51(8): p. 1868-1875.

8. A. Yıldırım and M. Çetin, Synthesis and evaluation of new long alkyl side chain acetamide, isoxazolidine and isoxazoline derivatives as corrosion inhibitors. Corrosion Science, 2008. 50(1): p. 155-165.

9. C. Hansson, L. Mammoliti, and B. Hope, Corrosion inhibitors in concrete—part I: the principles. Cement and concrete research, 1998. 28(12): p. 1775-1781.

10. A. Abdel-Gaber, et al., A natural extract as scale and corrosion inhibitor for steel surface in brine solution. Desalination, 2011. 278(1-3): p. 337-342.

11. M. Salasi, et al., The electrochemical behaviour of environment-friendly inhibitors of silicate and phosphonate in corrosion control of carbon steel in soft water media. Materials Chemistry and physics, 2007. 104(1): p. 183-190.

12. G. Blustein, et al., Zinc basic benzoate as eco-friendly steel corrosion inhibitor pigment for anticorrosive epoxy-coatings. Colloids and Surfaces A: Physicochemical and Engineering Aspects, 2006. 290(1-3): p. 7-18.

13. P. Bommersbach, et al., Formation and behaviour study of an environment-friendly corrosion inhibitor by electrochemical methods. Electrochimica Acta, 2005. 51(6): p. 1076-1084.

14. A. Lecante, et al., Anti-corrosive properties of S. tinctoria and G. ouregou alkaloid extracts on low carbon steel. Current Applied Physics, 2011. 11(3): p. 714-724.

15. I. Radojčić, et al., Natural honey and black radish juice as tin corrosion inhibitors. Corrosion Science, 2008. 50(5): p. 1498-1504.

16. R. Omar, P. Koparir, and M. Koparir, Synthesis of 1, 3-Thiazole derivatives. Indian Drugs, 2021. 1: p. 58.

17. S.M. Lashgari, et al., Synthesis of graphene oxide nanosheets decorated by nanoporous zeolite-imidazole (ZIF-67) based metal-organic framework with controlled-release corrosion inhibitor performance: Experimental and detailed DFT-D theoretical explorations. Journal of Hazardous Materials, 2021. 404: p. 124068.

18. A.K. Singh and M. Quraishi, The effect of some bis-thiadiazole derivatives on the corrosion of mild steel in hydrochloric acid. Corrosion Science, 2010. 52(4): p. 1373-1385.

19. A.Y. Musa, R.T. Jalgham, and A.B. Mohamad, Molecular dynamic and quantum chemical calculations for phthalazine derivatives as corrosion inhibitors of mild steel in 1 M HCl. Corrosion Science, 2012. 56: p. 176-183.

20. D.K. Yadav and M.A. Quraishi, Application of some condensed uracils as corrosion inhibitors for mild steel: gravimetric, electrochemical, surface morphological, UV–visible, and theoretical investigations. Industrial & engineering chemistry research, 2012. 51(46): p. 14966-14979.

21. M. Bobina, et al., Corrosion resistance of carbon steel in weak acid solutions in the presence of l-histidine as corrosion inhibitor. Corrosion Science, 2013. 69: p. 389-395.

22. H. El Sayed and S.A. Senior, QSAR of lauric hydrazide and its salts as corrosion inhibitors by using the quantum chemical and topological descriptors. Corrosion Science, 2011. 53(3): p. 1025-1034.

23. H. Zhao, et al., Quantitative structure–activity relationship model for amino acids as corrosion inhibitors based on the support vector machine and molecular design. Corrosion Science, 2014. 83: p. 261-271.

24. O. Rebaz, et al., Theoretical Determination of Corrosion Inhibitor Activities of Naphthalene and Tetralin. Gazi University Journal of Science, 2022: p. 1-1.

25. R.A. Omer, P. Koparir, and L.O. Ahmed, Characterization and Inhibitor Activity of Two Newly Synthesized Thiazole. Journal of Bio-and Tribo-Corrosion, 2022. 8(1): p. 1-12.

26. P. KOPARIR, et al., Synthesis, Characterization, and theoretical inhibitor study for (1E, 1'E)-2, 2'-thiobis (1-(3-mesityl-3-methylcyclobutyl) ethan-1-one) dioxime. El-Cezeri, 2020. 8(3): p. 1495-1510.

27. L. AHMED and O. Rebaz, Spectroscopic properties of Vitamin C: A theoretical work. Cumhuriyet Science Journal, 2020. 41(4): p. 916-928.

28. R.A. OMER, et al., Computational and spectroscopy study of melatonin. Indian Journal of Chemistry-Section B (IJC-B), 2021. 60(5): p. 732-741.

29. F. Bentiss, et al., On the relationship between corrosion inhibiting effect and molecular structure of 2, 5-bis (n-pyridyl)-1, 3, 4-thiadiazole derivatives in acidic media: Ac impedance and DFT studies. Corrosion Science, 2011. 53(1): p. 487-495.

30. I. Ahamad, R. Prasad, and M. Quraishi, Adsorption and inhibitive properties of some new Mannich bases of Isatin derivatives on corrosion of mild steel in acidic media. Corrosion Science, 2010. 52(4): p. 1472-1481.

31. I. Obot and Z. Gasem, Theoretical evaluation of corrosion inhibition performance of some pyrazine derivatives. Corrosion Science, 2014. 83: p. 359-366.

32. O. Rebaz, et al., Structure reactivity analysis for Phenylalanine and Tyrosine. Cumhuriyet Science Journal, 2021. 42(3): p. 576-585.

33. L. AHMED and O. Rebaz, The Role of the Various Solvent Polarities on Piperine Reactivity and Stability. Journal of Physical Chemistry and Functional Materials, 2021. 4(2): p. 10-16.

34. L.A. OMER and R.O. ANWER, Population Analysis and UV-Vis spectra of Dopamine Molecule Using Gaussian 09. Journal of Physical Chemistry and Functional Materials, 2020. 3(2): p. 48-58.

35. R.A. Omer, et al., Theoretical analysis of the reactivity of chloroquine and hydroxychloroquine. Indian Journal of Chemistry-Section A (IJCA), 2020. 59(12): p. 1828-1834.

36. O. Rebaz, et al., Computational determination the reactivity of salbutamol and propranolol drugs. Turkish Computational and Theoretical Chemistry, 2020. 4(2): p. 67-75.

37. L. AHMED and O. Rebaz, Computational Study on Paracetamol Drug. Journal of Physical Chemistry and Functional Materials, 2020. 3(1): p. 9-13.

38. L. AHMED and O. Rebaz, A theoretical study on Dopamine molecule. Journal of Physical Chemistry and Functional Materials, 2019. 2(2): p. 66-72.

39. R. Omer, et al., Synthesis, Characterization and DFT Study of 1-(3-Mesityl-3-methylcyclobutyl)-2-((4-phenyl-5-(thiophen-2-yl)-4H-1, 2, 4-triazol-3-yl) thio) ethan-1-one. Protection of Metals and Physical Chemistry of Surfaces, 2022: p. 1-13.

40. A.D. Becke, Density-functional thermochemistry. IV. A new dynamical correlation functional and implications for exact-exchange mixing. The Journal of chemical physics, 1996. 104(3): p. 1040-1046.

41. O. Rebaz, et al., Structural Analysis of Epinephrine by Combination of Density Functional Theory and Hartree-Fock Methods. El-Cezeri, 2022. 9(2): p. 760-776.

42. M. Beytur, et al., Synthesis, characterization and theoretical determination of corrosion inhibitor activities of some new 4, 5-dihydro-1H-1, 2, 4-Triazol-5-one derivatives. Heliyon, 2019. 5(6): p. e01809.

43. P. Koparir, et al., Synthesis, Characterization and Computational Analysis of Thiophene-2, 5-Diylbis ((3-Mesityl-3-Methylcyclobutyl) Methanone). Polycyclic Aromatic Compounds, 2022: p. 1-19.

44. O. Rebaz, et al., Impact of Solvent Polarity on the molecular properties of Dimetridazole. El-Cezeri, 2022. 9(2): p. 740-747.

45. T. Koopmans, Über die Zuordnung von Wellenfunktionen und Eigenwerten zu den einzelnen Elektronen eines Atoms. physica, 1934. 1(1-6): p. 104-113.

46. B.N. Plakhutin and E.R. Davidson, Koopmans' theorem in the restricted open-shell Hartree− Fock Method. 1. A variational approach. The Journal of Physical Chemistry A, 2009. 113(45): p. 12386-12395.

47. P. Koparir, et al., Theoretical determination of corrosion inhibitor activities of 4-allyl-5-(pyridin-4-yl)-4H-1, 2, 4-triazole-3-thiol-thione tautomerism. 2022.

48. E.P. Jesudason, et al., Synthesis, pharmacological screening, quantum chemical and in vitro permeability studies of N-Mannich bases of benzimidazoles through bovine cornea. European journal of medicinal chemistry, 2009. 44(5): p. 2307-2312.

49. H. Gökce and S. Bahçeli, A study on quantum chemical calculations of 3-, 4-nitrobenzaldehyde oximes. Spectrochimica Acta Part A: Molecular and Biomolecular Spectroscopy, 2011. 79(5): p. 1783-1793.

50. M.S. Masoud, et al., Synthesis, computational, spectroscopic, thermal and antimicrobial activity studies on some metal–urate complexes. Spectrochimica Acta Part A: Molecular and Biomolecular Spectroscopy, 2012. 90: p. 93-108.

51. R.G. Pearson, Absolute electronegativity and hardness: application to inorganic chemistry. Inorganic chemistry, 1988. 27(4): p. 734-740.

52. S. Chen, et al., Quantum chemical study of some benzimidazole and its derivatives as corrosion inhibitors of steel in HCl solution. Int. J. Electrochem. Sci, 2014. 9: p. 5400-5408.

53. Z. El Adnani, et al., DFT theoretical study of 7-R-3methylquinoxalin-2 (1H)-thiones (RH; CH3; Cl) as corrosion inhibitors in hydrochloric acid. Corrosion Science, 2013. 68: p. 223-230.

54. O. Rebaz, et al., Theoretical Analysis of the Reactivity of Carmustine and Lomustine Drugs. Journal of Physical Chemistry and Functional Materials, 2022. 5(1): p. 84-96.

55. E.C. Koch, Acid-Base Interactions in Energetic Materials: I. The Hard and Soft Acids and Bases (HSAB) Principle–Insights to Reactivity and Sensitivity of Energetic Materials. Propellants, Explosives, Pyrotechnics: An International Journal Dealing with Scientific and Technological Aspects of Energetic Materials, 2005. 30(1): p. 5-16.

56. S. Kaya, et al., Effect of some electron donor and electron acceptor groups on stability of complexes according to the principle of HSAB. Journal of New Results in Science, 2014. 3(4): p. 1-1.